Transfer induced compressive strain in graphene

Evidence from Raman spectroscopic mapping

Larsen, Martin Benjamin Barbour Spanget; Mackenzie, David; Caridad, Jose; Bøggild, Peter; Booth, Tim

Published in:
Microelectronic Engineering

Link to article, DOI:
10.1016/j.mee.2014.04.038

Publication date:
2014

Document Version
Peer reviewed version

Transfer induced compressive strain in graphene: Evidence from Raman spectroscopic mapping

Martin Benjamin B. S. Larsen[a], David M. A. Mackenzie[a], José M. Caridad[a], Peter Bøggild[a], Timothy J. Booth[a]
[a] DTU Nanotech, Ørsteds Plads 345 B, Kgs. Lyngby, 2800, Denmark
e-mail: martin.larsen@nanotech.dtu.dk, david.mackenzie@nanotech.dtu.dk, tim.booth@nanotech.dtu.dk, peter.boggild@nanotech.dtu.dk
Phone number: +45 4525 5788

Highlights

- We investigate the Raman spectrum of CVD graphene before and after transfer
- Comparison of transferred CVD graphene on SiO2 and exfoliated graphene using Raman spectroscopy

Keywords: CVD Graphene; Exfoliated Graphene; Graphene transfer; Raman mapping; Cu catalysts; Comparison.

3. Materials – nanomaterials for device fabrication

Abstract

We have used spatially resolved micro Raman spectroscopy to map the full width at half maximum (FWHM) of the graphene G-band and the 2D and G peak positions, for as-grown graphene on copper catalyst layers, for transferred CVD graphene and for micromechanically exfoliated graphene, in order to characterize the effects of a transfer process on graphene properties. Here we use the FWHM(G) as an indicator of the doping level of graphene, and the ratio of the shifts in the 2D and G bands as an indicator of strain. We find that the transfer process introduces an isotropic, spatially uniform, compressive strain in graphene, and increases the carrier concentration.

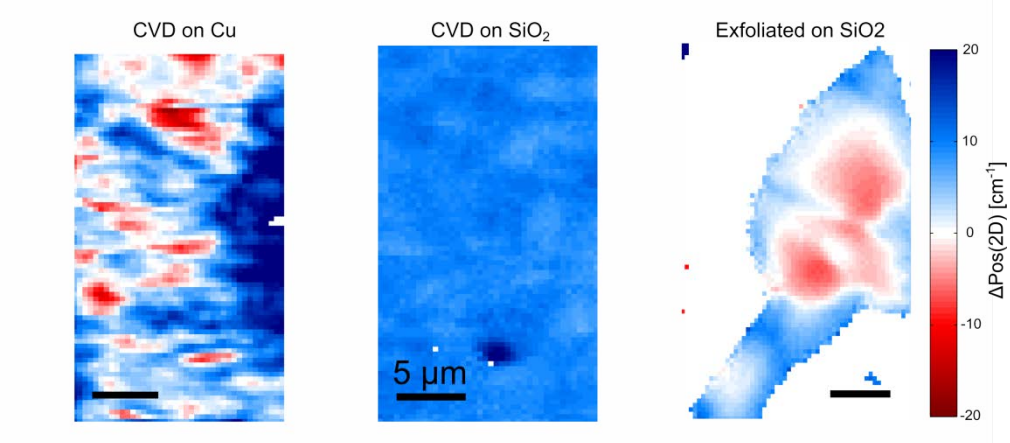

1. Introduction

Raman spectroscopy is a widely used technique for the non-destructive characterization of the properties of graphene [1][2]. The frequency, relative intensity, width, shape and position of characteristic peaks in the Raman spectrum of graphene provide information on the strain[4], doping[5] and presence of defects [3][6]. It is also possible to characterize the number of layers in the case of Bernal stacked graphene multilayers using the shape of the 2D peak [7]. The spatial variation of these properties can be mapped by scanning the excitation laser across the sample surface – this provides important information beyond that which can be obtained from single point spectra.

The interpretation of Raman spectra is complicated by the influence of the substrate supporting the graphene and the excitation energy used [1][7][8]. This is particularly relevant in the case of chemical vapour deposition (CVD) growth of graphene on metallic catalysts. In many practical applications, subsequent transfer of graphene to insulating substrates after growth is necessary. As it happens, variations in the Raman spectra obtained before and after transfer cannot immediately be ascribed to the influence of the particular substrate, to the effect of the transfer process or to the intrinsic properties of the graphene. Nevertheless, it would be useful to know the quality of graphene on insulator that can be expected from graphene on catalyst before transfer, and in particular whether the transfer process has a detrimental effect on the properties of the transferred graphene.

Here we use maps of the position of the 2D band and the G band, their shift direction and the full width at half maximum (FWHM) of the G band, in order to provide spatial information on the level of strain or doping in CVD grown graphene films on copper and transferred to oxidized silicon, and compare with mechanically exfoliated graphene layers on silicon dioxide.

2. Materials and Methods

Graphene was deposited in an Aixtron 4-inch Black Magic CVD system. The process starts with a low temperature annealing step at 500 degrees C with 1000 sccm H2 for 30 minutes and 25 mbar pressure, followed by a high temperature annealing step at 975 degrees C with the same gas flow rate and pressure. The system is then evacuated until a pressure of 0.5 mbar is reached and a CH_4 flowrate of 10 sccm for 5 minutes is introduced [3]. The catalyst substrate is a 4 inch silicon wafer with a 1 µm thick thermal oxide with a 1.5 µm thin sputtered copper layer on top; the copper deposition is done in a Polyteknik Cryofox physical vapor deposition system. Mechanically exfoliated graphene was produced following Refs [9][10]. The CVD graphene was transferred from the copper to a silicon wafer with a 90 nm SiO_2 layer, using electrochemical transfer [11].

The Raman characterization was carried out using a DXR Raman Microscope from Thermo Scientific, using three different excitation lasers, with 445 nm, 532 nm and 633 nm wavelength using a 100X objective. Excitation lasers were exchanged without moving the sample in order to produce maps of nearly identical regions for each excitation.

Raman peaks from individual spatial points were fitted with a single symmetrical Lorentzian function plus a linear background, using a least-squares regression adapted from [12]. In this way the relative intensity of the peaks, position and full-width at half maximum can be plotted for each point of the sample surface. Due to the self-limiting nature of CVD fabrication of graphene on a copper catalyst, we do not expect changes in the shape of the 2D peak due to AB stacked multilayers.

We do not observe G peak splitting in our datasets due to low values of strain here (<< 0.3%) and the probable absence of uni-axial strain [14].

3. Results

Figure 1 shows the FWHM(G) for each excitation wavelength and for the as-grown and transferred CVD graphene, as well as for mechanically exfoliated graphene. It can be seen that the FWHM(G) decreases after transfer of graphene from the catalytic growth substrate to an oxide layer (Fig.1 b-d vs. f-h). Small regions where FWHM(G) varies around 15 cm^{-1} indicate locally lower carrier concentrations for transferred graphene and exfoliated graphene (Fig.1 f-h, j-l). The FWHM(G) also shows comparable distribution for both transferred CVD graphene on oxide and exfoliated graphene. The measurements of the FWHM(G) for graphene on copper show broadening of the G band, particularly in the case of the 633 nm excitation (Fig.1 d).

Figure 2 shows the shift in the 2D (ΔPos(2D)) and G (ΔPos(G)) positions. While the shift in the 2D and G bands vary around zero for CVD graphene on copper and exfoliated graphene (Fig 2 a-c, j-l), transferred CVD graphene shows shifts towards larger wavenumbers for both the 2D and G bands (Fig. 2 d-f, m-o). The shifts in the 2D and G band positions are notably more uniform for CVD graphene on SiO_2 than for CVD graphene on copper and for exfoliated graphene on oxide. These trends are independent of the excitation laser used.

The ratio ΔPos(2D)/ ΔPos(G) of the peak shifts of 2D and G peaks is plotted in Fig. 3.. Wide variation in this ratio is seen for CVD graphene on copper and exfoliated graphene – in the latter case distinct ridges are observed in the flake, which potentially correspond to wrinkles or folds (e.g. Fig. 3 h). CVD graphene transferred to oxide shows a more uniform distribution of these values, and ΔPos(2D)/ΔPos(G) closer to ~ 2 (Fig. 3 d-f).

Figure 4 shows selected Raman spectra of neutral, doped, and strained regions on the same exfoliated graphene flake, at the indicated positions. The shift in the G and the 2D peaks indicated strain, but their intensities remain similar to that of neutral graphene. The doped graphene has a decreased 2D peak, while the G peak has narrowed compared to neutral graphene.

Poor signal to noise ratio in the 633 nm maps prevents adequate fitting of the peaks in the Raman spectra. We attribute the poor signal to noise to the fluorescence due to the interband transition in copper at around 650 nm [13]. Maps at the

445 nm and the 532 nm are indistinguishable within the spatial and spectral resolution of the spectrometer. The 445 nm laser shows higher sensitivity to DeltaPos(2D)/DeltaPos(G) for CVD graphene on Cu compared to the other two excitation energies.

In the case of CVD graphene transferred to SiO2 there is no significant variation in the FWHM(G) for the three different excitation energies. The charge puddles are consistently seen with all of the lasers. Differences in the maps can be ascribed to the spatial resolution of the different excitation lasers. For CVD graphene transferred to SiO2 we see a very similar level of strain with the 445 nm, the 532 nm and the 633 nm lasers, which we attribute to strain induced by the transfer process.

For exfoliated graphene on SiO2 all three laser show the same tendencies of the FWHM(G), but the signal to noise combined with the poor resolution of the 633 nm laser makes this laser less suited for mapping due to the very long collection times and spatial resolution obtained. The strain observed in exfoliated graphene on SiO2 is very similar for all three excitation energies.

4. Discussion

It is known that the doping level and the strain in graphene are reflected in changes of the 2D band and the G band from those expected for intrinsic graphene [4]. A FWHM(G) of ~ 15 cm^{-1} indicates carrier concentrations close to 0 [15], with a narrower FWHM of down to 8 cm^{-1} indicating greater doping. The 2D peak position enables the sign of the doping to be determined as well, since this peak upshifts in the case of hole doping, and downshifts for electron doping [5]. The effect of strain in suspended graphene has been also been studied – isotropic (biaxial) tensile strain results in downshifting of the G and 2D peaks, with the relative change in the position of the 2D and G bands of ~ 2 indicating strain rather than doping [4]. G-band splitting has been observed for uniaxial strains greater than +/- 0.3% [16], and a shift of this band to smaller or larger wavenumbers in the case of tensile or compressive strain respectively.

To summarize, where FWHM(G) is relatively small, doping is indicated, particularly where the ratio of the shifts is less than ~ 2. The 2D shift direction then indicates the type of doping. Where FWHM(G) is maximal, doping can be discounted, and the shifts in the 2D and G bands can be ascribed to strain. The ratio $\Delta 2D/\Delta G$ in this case should be ~ 2. The G shift direction then indicates whether the strain is tensile or compressive.

Our observations of the FWHM(G) show an overall decrease when CVD graphene is transferred to oxide. Exfoliated and transferred CVD graphene show similar micron scale “puddles” of lower carrier concentration. The FWHM(G) is distinctly wider for as-grown CVD graphene on copper, which likely represents the effects of charge transfer from the substrate. It is therefore not possible to ascribe the FWHM(G) wholly to the properties of the graphene in the case where it lies on a metal catalyst layer. The variation in the FWHM was similar between the exfoliated graphene and the CVD graphene on copper – however due to the uncertainties introduced by the substrate it is difficult to draw conclusions.

The Pos(2D) and Pos(G) for CVD graphene transferred to oxide both display less variation than is seen in CVD graphene on copper and exfoliated graphene. Additionally, the ratios of the band shifts, $\Delta Pos(2D)/\Delta Pos(G)$, also becomes more uniform and closer to ~ 2 for transferred CVD graphene. This indicates that the graphene peak variations observed originate from the effects of an isotropic strain introduced during the transfer process. This conclusion is supported by our observations of the $\Delta Pos(2D)/\Delta Pos(G)$ for exfoliated graphene, which show values close to ~ 2 around wrinkles, corresponding to high strain. CVD graphene grown on Cu and exfoliated graphene have similar variations in $\Delta Pos(2D)/\Delta Pos(G)$ over a few μm^2. The strain in exfoliated graphene is a result of the fabrication process – the strain in CVD graphene on copper results from the roughness of the copper surface and from the different thermal expansion coefficients of graphene and copper (Fig. 1a). Since the 2D and G peaks shift to larger wavenumbers and the ratio of these shifts is ~ 2, we can determine that our transfer process leads to compressive straining of the graphene.

Thus, either during the CVD growth or transfer process a uniform compressive strain is induced on the CVD graphene transferred to a SiO2 substrate. A further study has to be undertaken to decide whether this bi-axial strain is induced by the growth or the transfer process.

5. Conclusions

We have used spatially resolved Raman spectroscopy to map the full width at half maximum of the graphene G-band and the 2D and G peak positions, for as-grown graphene on copper catalyst layers, for transferred CVD graphene and for

micromechanically exfoliated graphene, in order to characterize the effects of a transfer process on the strain and doping level of graphene.

In general, it is challenging to distinguish between strain and doping in graphene using Raman spectroscopy *a priori* without explicitly introducing these through e.g. mechanical deformation or electrostatic gating. Additionally both strain and doping can vary spatially simultaneously. Here we use the FWHM(G) as an indicator of the doping level of graphene, and the ratio of the shifts in the 2D and G bands as evidence of strain.

We find that the transfer process introduces an isotropic compressive strain in graphene, which is also spatially uniform. Whilst this strain is mostly an undesirable property, the observed homogeneity could be an advantage in the production of devices where consistency over several hundred μm^2 is more important than having better but inconsistent electronic characteristics.

Relatively low carrier concentrations were observed for CVD graphene on copper, as evidenced by the FWHM(G). However, the transfer process had the effect of significantly increasing the doping level, as determined by a narrowing of the FWHM of the G-peak. However, the resulting doping level was consistent with the average level of doping in graphene exfoliated on identical oxide substrates. Both exfoliated and transferred CVD graphene showed similar several micron wide "puddles" of low doping which were similar to doping levels seen on CVD graphene on Cu. In fact, transferred graphene shows a generally lower doping than exfoliated graphene here, as evidenced by a FWHM(G) closer to 15 cm-1 in more areas.

The non-destructive mapping of properties of graphene is important as a control of quality and process consistency at each step of a graphene device production. The Raman spectrum of as-grown graphene on copper should not be considered to be representative of same graphene after transfer to oxidized silicon. Knowledge of the spatial variation of the doping and strain in CVD graphene over large areas will help to increase the consistency and reliability of the resulting devices produced. It is critical that the spatial variation of these properties is considered – point spectra are not adequate for complete characterization of the graphene quality, not even of single crystalline graphene.

References

[1] Sara D. Costa, Ariete Righi, Cristiano Fantini, Yufeng Hao, Carl Magnuson, Luigi Colombo, Rodney S. Ruoff, Marcos A. Pimenta. Resonant Raman spectroscopy of graphene grown on copper substrates. Solid State Communications 152, 1317–1320, 2011

[2] Tao, L.; Lee, J.; Holt, M.; Chou, H.; McDonnell, S. J.; Ferrer, D. A.; Babenco, M. G.; Wallace, R. M.; Banerjee, S. K.; Ruoff, R. S.; et al. Uniform Wafer-Scale Chemical Vapor Deposition of Graphene on Evaporated Cu (111) Film with Quality Comparable to Exfoliated Monolayer. Journal of Physical Chemistry C, 116, 24068–24074, 2012

[3] P. Klar, E. Lidorikis, A. Eckmann, I. A. Verzhbitskiy, A. C. Ferrari, and C. Casiraghi. Raman scattering efficiency of graphene. Physical Review B 87, 205435, 2013

[4] Jakob Zabel, Rahul R. Nair, Anna Ott, Thanasis Georgiou, Andre K. Geim, Kostya S. Novoselov, Cinzia Casiraghi. Raman Spectroscopy of graphene and bilayer under biaxial strain: bubbles and balloons. Nano Letters, 12, 617-621, 2012

[5] C. Casiraghia, S. Pisana, K. S. Novoselov, A. K. Geim, A. C. Ferrari. Raman fingerprint of charged impurities in graphene, Applied Physics Letters 91, 233108, 2007

[6] Ado Jorio, Erlon H. Martins Ferreira, Luiz G. Cançado, Carlos A. Achete and Rodrigo B. Capaz. Measuring Disorder in Graphene with Raman Spectroscopy, Physics and Applications of Graphene - Experiments, Dr. Sergey Mikhailov (Ed.), ISBN: 978-953-307-217-3, InTech, 2011.

[7] A. C. Ferrari. Raman spectroscopy of graphene and graphite: Disorder, electron–phonon coupling, doping and nonadiabatic effects. Solid State Communications 143, 47–57, 2007

[8] K. Sato, R. Saito, Y. Oyama a J. Jiang, L.G. Cancado, M.A. Pimenta, A. Jorio, Ge.G. Samsonidze, G. Dresselhaus, M.S. Dresselhaus. D-band Raman intensity of graphitic materials as a function of laser energy and crystallite size. Elsevier Science Volume 427, Issues 1–3, Pages 117–121, 18 August 2006

[9] K. S. Novoselov, A. K. Geim, S. V. Morozov, D. Jiang, Y. Zhang, S. V. Dubonos, I. V. Grigorieva and A. A. Firsov, Science 306, 666, 2004

[10] K. S. Novoselov, D. Jiang, F. Schedin, T. J. Booth, V. V. Khotkevich, S. V. Morozov and A. K. Geim, Proceedings of the National Academy of Sciences 102, 10451, 2005

[11] Libo Gao, Wencai Ren, Huilong Xu, Li Jin, Zhenxing Wang, Teng Ma, Lai-Peng Ma, Zhiyong Zhang, Qiang Fu, Lian-Mao Peng, Xinhe Bao, and Hui-Ming Chenga,. Repeated growth and bubbling transfer of graphene with millimetre-size single-crystal grains using platinum. Nature Communications, 3: 699, February 2012

[12] Tom O'Haver. Peak Fitter. www.mathworks.com/matlabcentral. 09 Apr 2009 (Updated 13 Sep 2013)

[13] L.M. Malarda, M.A. Pimentaa, G. Dresselhausb, M.S. Dresselhaus. Raman spectroscopy in graphene. Physics Reports, Volume 473, Issues 5–6, Pages 51–87, April 2009

[14] H. Ehrenreich and H. R. Philipp. Optical Properties of Ag and Cu. Physical Review, Vol 128 Number 4, November 1962

[15] Simone Pisana, Michele Lazzeri, Cinzia Casiraghi, Kostya S. Novoselov, A. K. Geim, Andrea C. Ferrari And Francesco Mauri. Breakdown of the adiabatic Born–Oppenheimer approximation in graphene. Nature Materials 6, March 2007

[16] T. M. G. Mohiuddin, A. Lombardo, R. R. Nair, A. Bonetti, G. Savini, R. Jalil, N. Bonini, D. M. Basko, C. Galiotis, N. Marzari, K. S. Novoselov, A. K. Geim, and A. C. Ferrari. Uniaxial strain in graphene by Raman spectroscopy: G peak splitting, Grüneisen parameters, and sample orientation. Physical Review B 79, 205433, 2009.

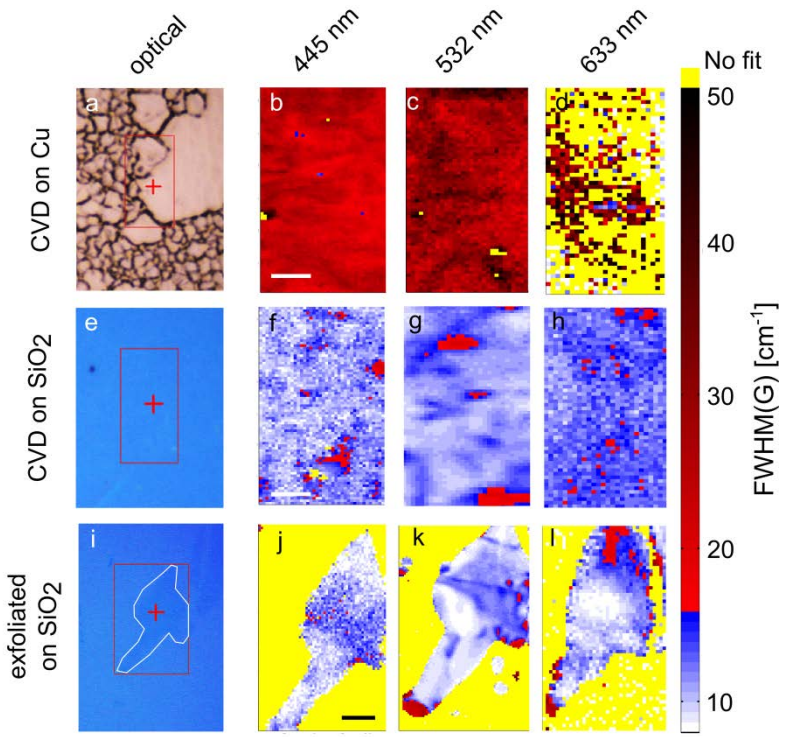

Figure 1 shows optical micrographs and the Raman FWHM(G) for CVD graphene on Cu (a-d), CVD graphene transferred to SiO_2 (e-h) and for exfoliated graphene on SiO_2 (i-l) for three different laser excitation wavelengths. The yellow color corresponds to no fitting, meaning no graphene or too poor signal to noise. The optical images as well as the Raman maps are collected with a 100x objective; the scale bars correspond to 5 µm. The map for CVD graphene on Cu is not considered due to poor signal to noise, but is added for consistency.

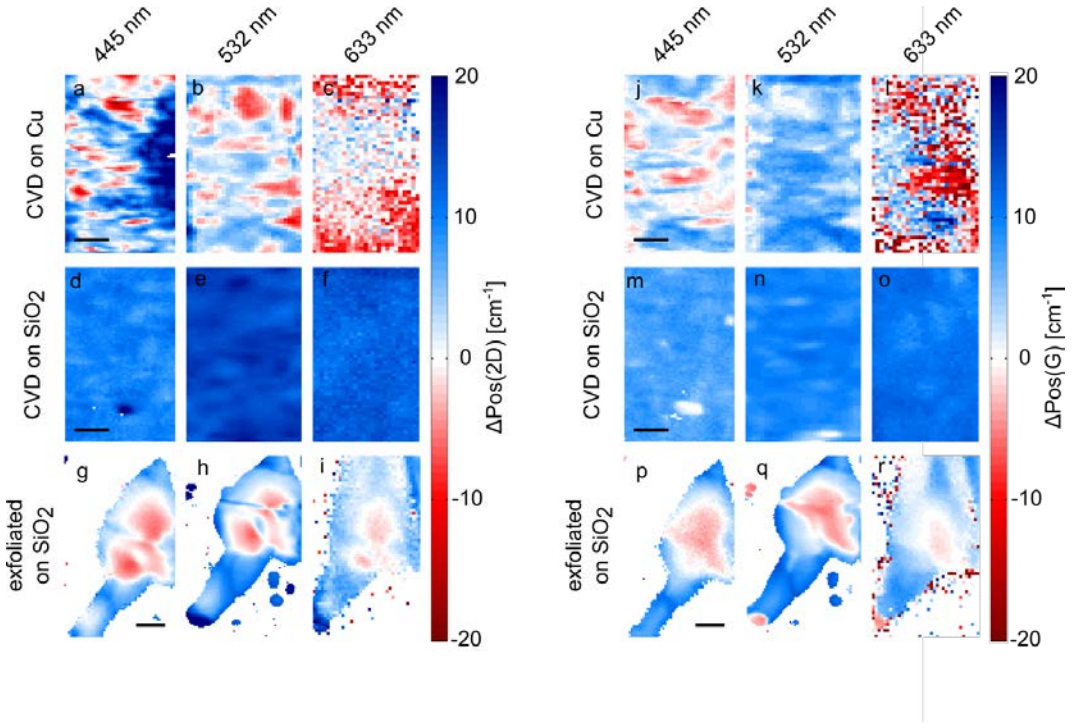

Figure 2 shows the relative shift in the 2D (a-i) and G (j-r) peak positions for CVD graphene on Cu, CVD graphene transferred to SiO_2 and exfoliated graphene on SiO_2. The shift is found as the measured values minus the theoretical values of 1588 cm-1 for the G peak and 2640 cm-1, 2675 cm-1 and 2720 cm-1 for 445 nm, 532 nm, and 633 nm [13].

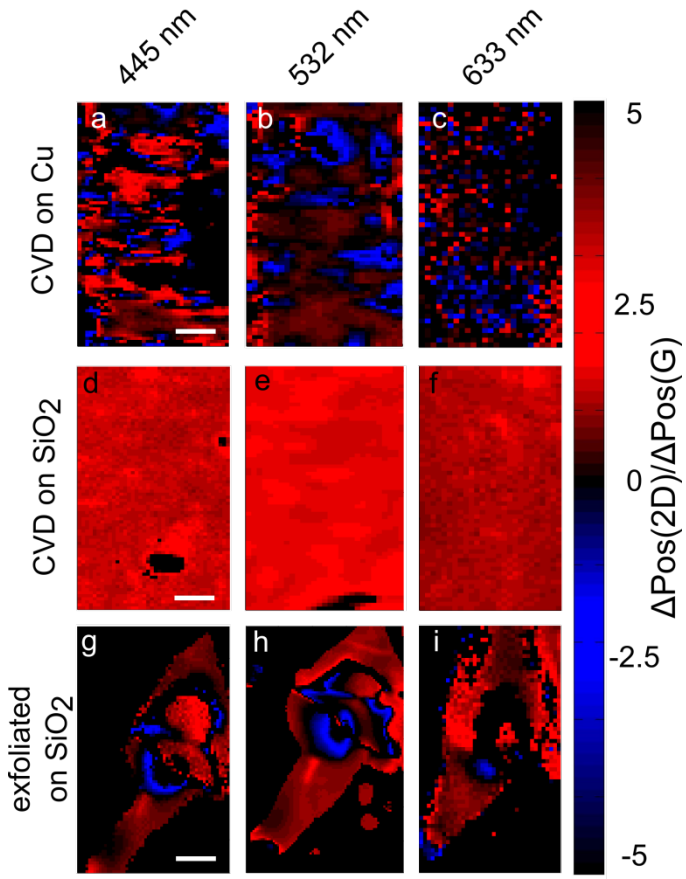

Figure 3 shows the ratio between the 2D peak shift and the G peak shift for CVD graphene on Cu(a-c), CVD graphene transferred to SiO_2(d-f) and exfoliated graphene on SiO_2(g-i) for the three laser wavelengths. The blue and red colors indicate regions of high strain, whereas the black regions indicate low to zero strain in the graphene films. The map for CVD graphene on Cu is not considered due to poor signal to noise, but is added for consistency.

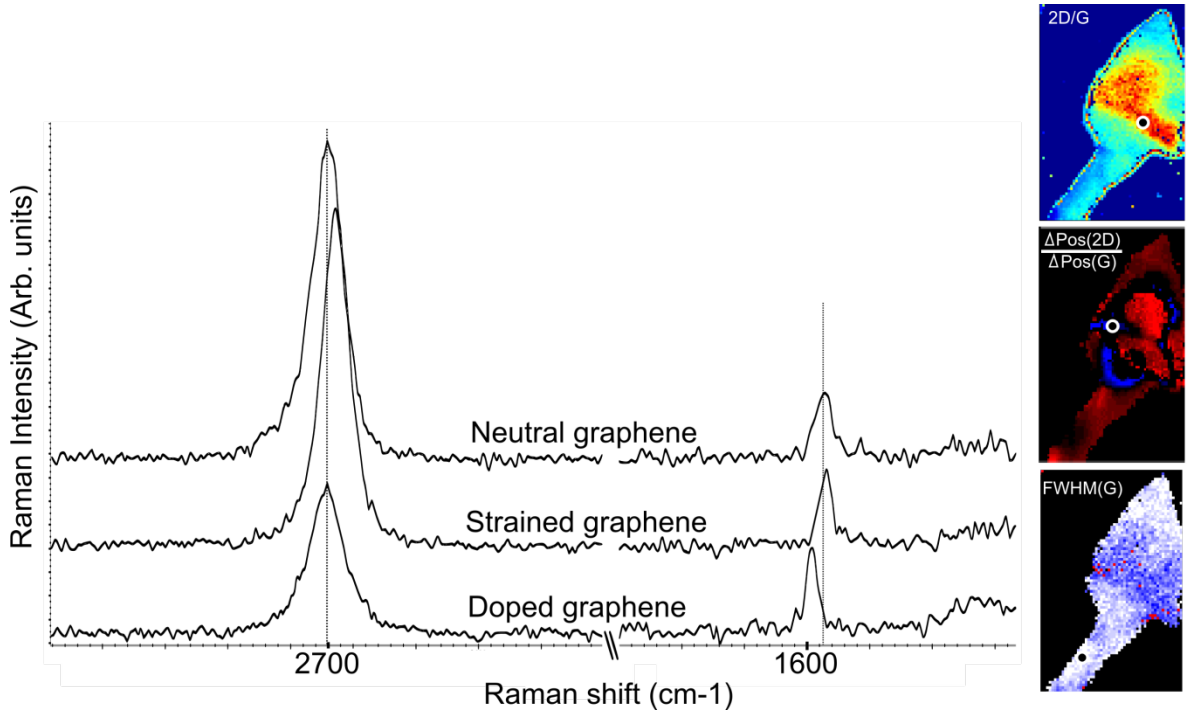

Figure 4 shows a raw spectrum of neutral graphene, doped graphene and strained graphene. The doped and strained spectra are extracted in regions where there is only one influence on the Raman spectrum, e.g. the strained graphene is not doped etc. The dotted lines are to guide the eye.